Pramana – J. Phys. (2019) 93:34
https://doi.org/10.1007/s12043-019-1781-8

Peristaltic transport of Jeffrey fluid in a rectangular duct through a porous medium under the effect of partial slip: An application to upgrade industrial sieves/filters

R ELLAHI[1,2,*], F HUSSAIN[2,3], F ISHTIAQ[2] and A HUSSAIN[4]

[1]Center for Modeling & Computer Simulation, Research Institute, King Fahd University of Petroleum & Minerals, Dhahran 31261, Saudi Arabia
[2]Department of Mathematics & Statistics, Faculty of Basic and Applied Sciences, International Islamic University, Islamabad 44000, Pakistan
[3]Department of Mathematics, Faculty of Arts and Basic Sciences, Balochistan University of Information Technology, Engineering and Management Sciences, Quetta 87300, Pakistan
[4]Department of Mechanical Engineering, Balochistan University of Information Technology, Engineering and Management Sciences, Quetta 87300, Pakistan
*Corresponding author. E-mail: rellahi@alumni.ucr.edu, rahmatellahi@yahoo.com

MS received 11 June 2018; revised 10 January 2019; accepted 30 January 2019; published online 14 June 2019

Abstract. The peristaltic transport of Jeffrey fluid through the rectangular duct is investigated. The effect of porosity under the influence of partial slip is also taken into consideration. The equations describing the flow transport along with boundary conditions are first made dimensionless using appropriate transformations and are then solved to get the exact solutions. The role of pressure rise generated by the fluid is also presented. The obtained results are examined graphically through pertinent parameters affecting the flow. The streamlines have also been displayed to analyse the trapping phenomenon.

Keywords. Peristaltic; Jeffrey fluid; porous medium; partial slip; trapping phenomenon.

PACS Nos 47.50.−d; 47.10.A

1. Introduction

Nowadays, design and improvement of industrial strainers are the challenging issues facing the chemical, petroleum and pharmaceutical industries, especially filtering or straining out unwanted impurities from fluids present in products like medical syrups. Similarly, recycling of industrial wastes during the manufacturing to maintain the environment clean, healthy and less harmful depends highly on the pores and permeability of sieves or filters. In addition, designing gold pans, by mining and geological enthusiasts, to maximise the extraction of gold with least wastage is another challenging job. Moreover, it is well established that the main natural resources of fresh water are springs, fountains, rivers and lakes. All rivers do not flow above the ground throughout their journey from their sources to estuaries. Sometimes, a river vanishes beneath the ground at one place and emerges above the ground at some other place. How does this underground flow take place? Flow of all sort of fluids (liquids and gases) beneath the crust through sands, soil particles and aquifers is caused by the 'porosity of the matter' or 'void friction'. The porosity of a rock or a matter is a measure of its ability to hold or allow fluids to pass through it. In the rocks, there are tiny spaces that hold oil, gas, etc. Quantity or capacity of porosity for any material lies between 0% and 100%; for instance, the sandstone consists of 8% of the void friction. This means that 92% of its composition is solid rock and 8% is an open space, permitting fluids to pass through. In addition, the movement of waves along the flexible walls of any channel is basically the genesis of any peristaltic flow. The transport of fluids from one place to another in a body follows the mechanism/principle of peristaltic pumping. Moreover, peristaltic flows have a significant function in the practical applications of various biomedical apparatuses such as heart–lung machines, etc. Thorough investigations of the biofluids help physicians and surgeons to diagnose various diseases in humans, which are mainly due to the non-Newtonian nature of fluids, such as blood. Flow of non-Newtonian fluids through the porous

medium has always attracted the geologists because of their interesting behaviours. Therefore, a number of research works are easily available for the young and new learners, in which the veteran scientists and engineers have employed their unique innovation and skills, with their own perspective, to achieve their desired goals. It is well-known that Latham [1] is considered to be the pioneer who introduced the concept of peristalsis. Various theoretical and experimental attempts have been made to apprehend the phenomenon of peristaltic motion [1] in diverse situations. Among these, the early literature is presented by Shapiro *et al* [2]. Most recently, Mahmoud *et al* [3] have successfully applied the effects of magnetohydrodynamics (MHD) on peristaltic motion of Jeffrey fluid passing through porous medium in an asymmetric channel by means of Adomian decomposition method. An MHD peristaltic flow through porous medium, further undergoing the effects of slip, is reported by Mekheimer *et al* [4] for moderately large Reynolds number. They obtained series solution by the regular perturbation method. Vajravelu *et al* [5] analysed the heat transfer in a stratum comprising tiny holes of Jeffrey fluid. Elmaboud *et al* [6] studied the second-grade fluid peristaltically moving through porous medium. Governing partial differential equations are solved up to second order by considering the perturbation techniques. Khan *et al* [7] succeeded in obtaining an accurate solution of Jeffrey fluid in a channel lacking absolute symmetry. In addition, the peristaltic motion of the fluid, porosity and varying viscosity of the fluid have been brought under attention, as well. Nadeem *et al* [8] obtained an analytic solution for the problem caused by the impacts of MHD on Maxwell fluid resisted by the permeable medium. Recently, Moatimid *et al* [9] reported instability analysis in cylindrical sheets over porous media. The peristaltic fluid flow through porous medium in a cylindrical tube is presented by Shehawey and El Sebai [10]. The simultaneous effects of MHD and slip condition on peristaltic flow of Newtonian fluid are examined by Ebaid [11]. Khan *et al* [12] presented analytical results on peristaltically propagating flow of non-Newtonian fluid through a curved channel under magnetic effects. Some noteworthy investigations on peristaltic flow, porous medium and slip can be seen from [13–32].

A useful contribution to see the effects of partial slip condition coupled with porous medium hindering the peristaltic movement of Jeffrey fluid in a duct of rectangular cross-section is offered in this study. The available literature bear witness that the reported idea in this article is not yet available in the existing literature. Therefore, in order to bridge this gap, an attempt is made to analyse the peristaltic flow of Jeffrey fluid by using the assumption of long wavelength and low Reynolds number. The exact solutions are obtained by the method of separation of variables. In addition, the expression for stream functions is obtained numerically. Graphical behaviour of important parameters has also been discussed and displayed.

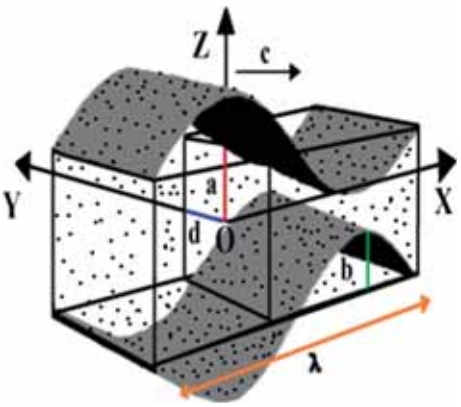

Figure 1. Geometry of the problem.

2. Formalism

An incompressible Jeffrey fluid passing through a duct of rectangular shape due to the peristaltic waves created by both the flexible axial walls having the channel width $2d$, height $2a$, constant speed c, amplitude b and wavelength λ as shown in figure 1 is considered:

$$\bar{Z} = \bar{H}(\bar{X}, \bar{t}) = \pm\bar{a} \pm \bar{b}\cos\left(\frac{2\pi\left(\bar{X} - \bar{c}\bar{t}\right)}{\bar{\lambda}}\right). \tag{1}$$

The resulting sets of equations of the problem under consideration in the components form are given below [33]:

$$\frac{\partial\bar{U}}{\partial\bar{X}} + \frac{\partial\bar{W}}{\partial\bar{Z}} = 0, \tag{2}$$

$$\frac{\partial\bar{U}}{\partial\bar{t}} + \bar{U}\frac{\partial\bar{U}}{\partial\bar{X}} + \bar{W}\frac{\partial\bar{U}}{\partial\bar{Z}} = \frac{1}{\bar{\rho}}\left(\frac{\partial\bar{S}_{\bar{X}\bar{X}}}{\partial\bar{X}} + \frac{\partial\bar{S}_{\bar{X}\bar{Y}}}{\partial\bar{Y}} + \frac{\partial\bar{S}_{\bar{X}\bar{Z}}}{\partial\bar{Z}} - \frac{\partial\bar{P}}{\partial\bar{X}} - \frac{\bar{\mu}}{\bar{K}}\bar{U}\right), \tag{3}$$

$$0 = \frac{1}{\bar{\rho}}\left(\frac{\partial\bar{S}_{\bar{Y}\bar{X}}}{\partial\bar{X}} + \frac{\partial\bar{S}_{\bar{Y}\bar{Y}}}{\partial\bar{Y}} + \frac{\partial\bar{S}_{\bar{Y}\bar{Z}}}{\partial\bar{Z}} - \frac{\partial\bar{P}}{\partial\bar{Y}}\right), \tag{4}$$

$$\frac{\partial\bar{W}}{\partial\bar{t}} + \bar{U}\frac{\partial\bar{W}}{\partial\bar{X}} + \bar{W}\frac{\partial\bar{W}}{\partial\bar{Z}} = \frac{1}{\bar{\rho}}\left(\frac{\partial\bar{S}_{\bar{Z}\bar{X}}}{\partial\bar{X}} + \frac{\partial\bar{S}_{\bar{Z}\bar{Y}}}{\partial\bar{Y}} + \frac{\partial\bar{S}_{\bar{Z}\bar{Z}}}{\partial\bar{Z}} - \frac{\partial\bar{P}}{\partial\bar{Z}} - \frac{\bar{\mu}}{\bar{K}}\bar{W}\right), \tag{5}$$

where $\bar{\rho}$ is the density, $\bar{\mu}$ is the viscosity, $\bar{P}$ is the pressure, $\bar{K}$ is the permeability and $\bar{t}$ is the time. The stress tensor of the Jeffrey fluid $\bar{S}$ is defined as

$$\bar{S} = \frac{\bar{\mu}(\dot{\bar{\Upsilon}} + \lambda_2 \ddot{\bar{\Upsilon}})}{\lambda_1 + 1}. \tag{6}$$

Here, λ_2 is the retardation time, whereas $\dot{\bar{\Upsilon}}$ represents the shear rate and is expressed as

$$\dot{\bar{\Upsilon}} = \nabla \bar{V} + [\nabla \bar{V}]^T. \tag{7}$$

Dot shows its time derivative. Boundary conditions related to this problem are as follows:

$$\text{(i) } \bar{U}\left(\bar{X}, \bar{Y}, \bar{Z}\right) = 0 \quad \text{when} \quad \pm d = \bar{Y}, \tag{8}$$

$$\text{(ii) } \bar{U}_{\text{wall}} + \frac{l}{\lambda_1 + 1}\frac{\partial \bar{U}}{\partial \bar{Z}} = \bar{U}\left(\bar{X}, \bar{Y}, \bar{Z}\right) \text{ when } -\bar{H}\left(\bar{X}, \bar{t}\right) = \bar{Z}, \tag{9}$$

$$\text{(iii) } \bar{U}_{\text{wall}} - \frac{l}{\lambda_1 + 1}\frac{\partial \bar{U}}{\partial \bar{Z}} = \bar{U}\left(\bar{X}, \bar{Y}, \bar{Z}\right) \text{ when } \bar{H}\left(\bar{X}, \bar{t}\right) = \bar{Z}. \tag{10}$$

Let c be the constant velocity of the wave frame that is in motion with respect to the fixed frame. Then by using the following transformation

$$\bar{X} - \bar{c}\bar{t} = \bar{x}, \quad \bar{Z} = \bar{z}, \quad \bar{p}(\bar{x}, \bar{z}) = \bar{P}\left(\bar{X}, \bar{Z}, \bar{t}\right),$$
$$\bar{Y} = \bar{y}, \quad \bar{W} = \bar{w}, \quad \bar{U} - \bar{c} = \bar{u} \tag{11}$$

along with the subsequent non-dimensional variables

$$\frac{\bar{x}}{\bar{\lambda}} = x, \quad \frac{\bar{y}}{\bar{d}} = y, \quad \frac{\bar{z}}{\bar{a}} = z, \quad \frac{\bar{u}}{\bar{c}} = u, \quad \frac{\bar{w}}{\bar{c}\bar{\delta}} = w,$$
$$\beta_1 = \frac{l}{\bar{a}}, \quad \frac{\bar{c}\bar{t}}{\bar{\lambda}} = t, \quad \frac{\bar{H}}{\bar{a}} = h, \quad \bar{\delta} = \frac{\bar{a}}{\bar{\lambda}},$$
$$\beta = \frac{\bar{a}}{\bar{d}}, \quad \text{Re} = \frac{\bar{\rho}\bar{c}\bar{\delta}\bar{a}}{\bar{\mu}}, \quad k = \frac{\bar{K}}{\bar{a}^2}, \quad \frac{\bar{b}}{\bar{a}} = \phi, \quad \frac{\bar{p}\bar{a}^2}{\bar{\mu}\bar{c}\bar{\lambda}} = p,$$
$$S_{xx} = \frac{\bar{a}}{\bar{\mu}\bar{c}}\bar{S}_{\bar{x}\bar{x}}, \quad S_{xz} = \frac{\bar{a}}{\bar{\mu}\bar{c}}\bar{S}_{\bar{x}\bar{z}},$$
$$S_{xy} = \frac{\bar{d}}{\bar{\mu}\bar{c}}\bar{S}_{\bar{x}\bar{y}}, \quad S_{yz} = \frac{\bar{d}}{\bar{\mu}\bar{c}}\bar{S}_{\bar{y}\bar{z}},$$
$$S_{yy} = \frac{\bar{\lambda}}{\bar{\mu}\bar{c}}\bar{S}_{\bar{y}\bar{y}}, \quad S_{zz} = \frac{\bar{\lambda}}{\bar{\mu}\bar{c}}\bar{S}_{\bar{z}\bar{z}} \tag{12}$$

in eqs (2)–(5) and (8)–(10) under the constraint of low Reynolds number and long wavelength, we eventually end up with the following equation:

$$\frac{\partial^2 u}{\partial y^2} + \frac{1}{\beta^2}\frac{\partial^2 u}{\partial z^2} - \left(\frac{\lambda_1 + 1}{\beta^2 k}\right)u = \frac{\lambda_1 + 1}{\beta^2}\left(\frac{\mathrm{d}p}{\mathrm{d}x} + \frac{1}{k}\right), \tag{13}$$

$$\text{(i) } u(x, y, z) = -1 \quad \text{when } \pm 1 = y, \tag{14}$$

$$\text{(ii) } u(x, y, z) = -1 - \left(\frac{\beta_1}{\lambda_1 + 1}\right)\frac{\partial u}{\partial z} \text{ when } z = 1 + \phi\cos(2\pi x), \tag{15}$$

$$\text{(iii) } u(x, y, z) = -1 + \left(\frac{\beta_1}{\lambda_1 + 1}\right)\frac{\partial u}{\partial z} \text{ when } z = -1 - \phi\cos(2\pi x), \tag{16}$$

where β is the aspect ratio, β_1 is the slip parameter, λ_1 is the Jeffrey parameter, l is the characteristic length and ϕ is the amplitude ratio.

3. Solutions of the problem

This section is devoted to obtain the analytical results of non-dimensional system of equations. As to find the solution of non-homogeneous partial differential equation given in eq. (13), subject to the corresponding boundary conditions (14) to (16) is not an easy task. It is therefore, more appropriate that first eq. (13) should be reduced to homogeneous partial differential equation by using the following transformation [34]

$$u(x, y, z) = \bar{u}_1(x, y, z) + \bar{u}_2(y). \tag{17}$$

In view of eq. (17), eqs (13)–(16) take the following forms:

$$\frac{\partial^2 \bar{u}_1}{\partial y^2} + \frac{1}{\beta^2}\frac{\partial^2 \bar{u}_1}{\partial z^2} - \left(\frac{\lambda_1 + 1}{\beta^2 k}\right)\bar{u}_1 = 0, \tag{18}$$

$$\frac{\mathrm{d}^2 \bar{u}_2}{\mathrm{d}y^2} - \left(\frac{\lambda_1 + 1}{\beta^2 k}\right)\bar{u}_2 = \left(\frac{\lambda_1 + 1}{\beta^2}\right)\left(\frac{\mathrm{d}p}{\mathrm{d}x} + \frac{1}{k}\right), \tag{19}$$

$$\text{(i) } \bar{u}_1(x, y, z) = 0 \quad \text{when } y = \pm 1, \tag{20}$$

$$\text{(ii) } \bar{u}_1(x, y, z) + \frac{\beta_1}{\lambda_1 + 1}\frac{\partial \bar{u}_1}{\partial z} = -1 - \bar{u}_2(y) \text{ when } z = h(x), \tag{21}$$

$$\text{(iii) } \bar{u}_1(x, y, z) - \frac{\beta_1}{\lambda_1 + 1}\frac{\partial \bar{u}_1}{\partial z} = -1 - \bar{u}_2(y) \text{ when } z = -h(x), \tag{22}$$

$$\text{(iv) } \bar{u}_2(y) = -1 \quad \text{when } y = \pm 1. \tag{23}$$

The solutions of eqs (18) and (19) are subject to conditions given in eqs (20)–(23). Therefore, we, respectively, obtain the following equations:

$$\bar{u}_1 = \frac{32\,k\frac{\mathrm{d}p}{\mathrm{d}x}(1+\lambda_1)^2\cos\left(\frac{\pi y}{2}\right)\cosh\left(z\sqrt{\frac{k(\pi\beta)^2+4\lambda_1+4}{4k}}\right)}{\pi(k\pi^2\beta^2+4\lambda_1+4)\times\left\{\begin{array}{l}2(1+\lambda_1)\cosh\left((1+\phi\cos 2\pi x)\sqrt{\frac{k(\pi\beta)^2+4\lambda_1+4}{4k}}\right)\\ +\beta_1\sqrt{\frac{k(\pi\beta)^2+4\lambda_1+4}{4k}}\sinh\left((1+\phi\cos 2\pi x)\sqrt{\frac{k(\pi\beta)^2+4\lambda_1+4}{4k}}\right)\end{array}\right\}} \tag{24}$$

and

$$\bar{u}_2 = -1 - k\frac{\mathrm{d}p}{\mathrm{d}x}\left[1-\operatorname{sech}\left(\sqrt{\frac{1+\lambda_1}{\beta^2 k}}\right)\cosh\left(\sqrt{\frac{1+\lambda_1}{\beta^2 k}}\,y\right)\right]. \tag{25}$$

Thus, the general solution of eq. (13) can be written as

$$u = \left\{+\frac{k\frac{\mathrm{d}p}{\mathrm{d}x}\left(\operatorname{sech}\left(\sqrt{\frac{1+\lambda_1}{\beta^2 k}}\right)\cosh\left(\sqrt{\frac{1+\lambda_1}{\beta^2 k}}\,y\right)-1\right)-1}{\pi(k\pi^2\beta^2+4\lambda_1+4)\times\left\{\begin{array}{l}2(1+\lambda_1)\cosh\left((1+\phi\cos 2\pi x)\sqrt{\frac{k(\pi\beta)^2+4\lambda_1+4}{4k}}\right)\\ +\beta_1\sqrt{\frac{k(\pi\beta)^2+4\lambda_1+4}{4k}}\sinh\left((1+\phi\cos 2\pi x)\sqrt{\frac{k(\pi\beta)^2+4\lambda_1+4}{4k}}\right)\end{array}\right\}}\right. \times \left\{32\,k\frac{\mathrm{d}p}{\mathrm{d}x}(1+\lambda_1)^2\cos\left(\frac{\pi y}{2}\right)\cosh\left(z\sqrt{\frac{k(\pi\beta)^2+4\lambda_1+4}{4k}}\right)\right\}. \tag{26}$$

The volumetric flow rate of Jeffrey fluid can be calculated by

$$\bar{q} = \int_0^1\int_0^{h(x)} u(x,y,z)\mathrm{d}z\,\mathrm{d}y. \tag{27}$$

Finally, one can achieve it as

$$\bar{q} = \left\{\begin{array}{l}128\,\frac{\mathrm{d}p}{\mathrm{d}x}(1+\lambda_1)^{3/2}-(1+\phi\cos 2\pi x)\left\{\left(1+k\frac{\mathrm{d}p}{\mathrm{d}x}\right)\sqrt{1+\lambda_1}-k^{3/2}\frac{\mathrm{d}p}{\mathrm{d}x}\beta\tanh\left(\sqrt{\frac{1+\lambda_1}{k\beta^2}}\right)\right\}\\ \times\left\{\pi^2\left(\frac{k(\pi\beta)^2+4\lambda_1+4}{k}\right)^{3/2}\left(2\coth\left((1+\phi\cos 2\pi x)\sqrt{\frac{k(\pi\beta)^2+4\lambda_1+4}{4k}}\right)+\sqrt{\frac{\beta_1^2\,(k(\pi\beta)^2+4\lambda_1+4)}{k(1+\lambda_1)^2}}\right)\right\}\\ \hline \sqrt{1+\lambda_1}\left\{\pi^2\left(\frac{k(\pi\beta)^2+4\lambda_1+4}{k}\right)^{3/2}\left(2\coth\left((1+\phi\cos 2\pi x)\sqrt{\frac{k(\pi\beta)^2+4\lambda_1+4}{4k}}\right)+\sqrt{\frac{\beta_1^2(k(\pi\beta)^2+4\lambda_1+4)}{k(1+\lambda_1)^2}}\right)\right\}\end{array}\right. . \tag{28}$$

In the same way, the average volumetric flow rate Q can be obtained as

$$Q = \left\{\begin{array}{l}128\,\frac{\mathrm{d}p}{\mathrm{d}x}(1+\lambda_1)^{3/2}-\left[\sqrt{1+\lambda_1}+(1+\phi\cos 2\pi x)\left\{\left(1+k\frac{\mathrm{d}p}{\mathrm{d}x}\right)\sqrt{1+\lambda_1}-k^{3/2}\frac{\mathrm{d}p}{\mathrm{d}x}\beta\tanh\left(\sqrt{\frac{1+\lambda_1}{k\beta^2}}\right)\right\}\right]\\ \times\left\{\pi^2\left(\frac{k(\pi\beta)^2+4\lambda_1+4}{k}\right)^{3/2}\left(2\coth\left((1+\phi\cos 2\pi x)\sqrt{\frac{k(\pi\beta)^2+4\lambda_1+4}{4k}}\right)+\sqrt{\frac{\beta_1^2\,(k(\pi\beta)^2+4\lambda_1+4)}{k(1+\lambda_1)^2}}\right)\right\}\\ \hline \sqrt{1+\lambda_1}\left\{\pi^2\left(\frac{k(\pi\beta)^2+4\lambda_1+4}{k}\right)^{3/2}\left(2\coth\left((1+\phi\cos 2\pi x)\sqrt{\frac{k(\pi\beta)^2+4\lambda_1+4}{4k}}\right)+\sqrt{\frac{\beta_1^2(k(\pi\beta)^2+4\lambda_1+4)}{k(1+\lambda_1)^2}}\right)\right\}\end{array}\right. . \tag{29}$$

The expression for pressure gradient in view of eq. (29) can be easily calculated as

$$\frac{\mathrm{d}p}{\mathrm{d}x}=\left\{\begin{array}{l}\pi^2(1+\lambda_1)(Q+\phi\cos(2\pi x))\left(k\pi^2\beta^2+4\lambda_1+4\right)^{3/2}\\ \times\left\{\begin{array}{l}2\sqrt{k}\,(1+\lambda_1)\cosh\left((1+\phi\cos(2\pi x))\sqrt{\frac{k\pi^2\beta^2+4\lambda_1+4}{4k}}\right)\\ +\beta_1\,\sinh\left((1+\phi\cos(2\pi x))\sqrt{\frac{k\pi^2\beta^2+4\lambda_1+4}{4k}}\right)\sqrt{k\pi^2\beta^2+4\lambda_1+4}\end{array}\right\}\\ \hline 128\,k^2(1+\lambda_1)^3\sinh\left((1+\phi\cos(2\pi x))\sqrt{\frac{k\pi^2\beta^2+4\lambda_1+4}{4k}}\right)+k\pi^2(1+\phi\cos(2\pi x))\\ \times\left(k\pi^2\beta^2+4\lambda_1+4\right)^{3/2}\left(k\beta\sqrt{\frac{1+\lambda_1}{k}}\tanh\left(\sqrt{\frac{1+\lambda_1}{k\beta^2}}\right)-\lambda_1-1\right)\\ \times\left\{\begin{array}{l}2\sqrt{k}\,(1+\lambda_1)\cosh\left((1+\phi\cos(2\pi x))\sqrt{\frac{k\pi^2\beta^2+4\lambda_1+4}{4k}}\right)\\ +\beta_1\,\sinh\left((1+\phi\cos(2\pi x))\sqrt{\frac{k\pi^2\beta^2+4\lambda_1+4}{4k}}\right)\sqrt{k}\pi^2\beta^2+4\lambda_1+4\end{array}\right\}\end{array}\right.. \tag{30}$$

Using the routine calculation, the pressure rise can be obtained by

$$\Delta p=\int_0^1\frac{\mathrm{d}p}{\mathrm{d}x}\mathrm{d}x. \tag{31}$$

4. Results and discussion

This section details the parametric study with the help of graphs, which have a greater influence on the fluid. Hence, causing the change in the trend of the flow by means of key parameters that explain how they really prompt the relative changes in the fluid's behaviour, by varying them. The most significant parameters in this study are amplitude ratio ϕ, volumetric flow rate Q, aspect ratio β, Jeffrey fluid parameter λ_1, slip parameter β_1 and the porosity parameter k.

Figures 2–6 show how pressure gradient reacts against the variation for different numerical values of β, λ_1, β_1, k and Q. It is worth noticing that the pressure gradient

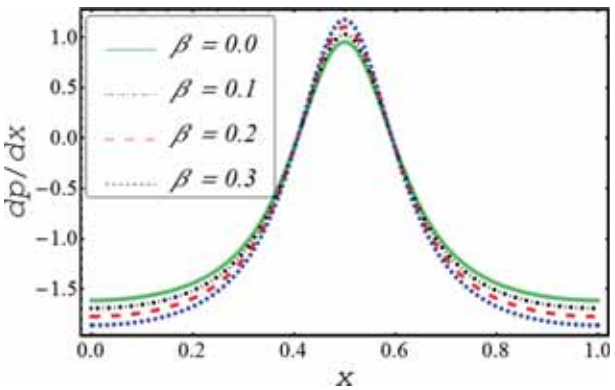

Figure 2. Variation in pressure gradient for β.

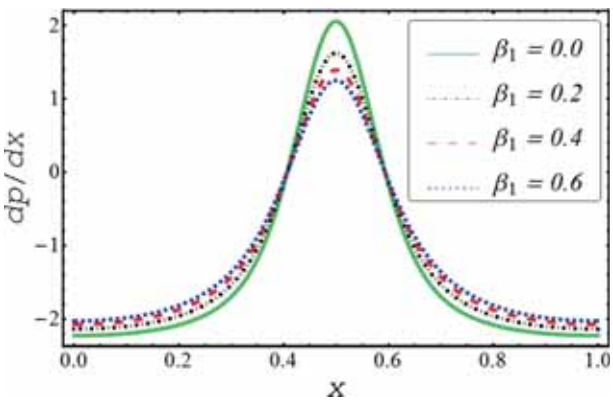

Figure 3. Variation in pressure gradient for β_1.

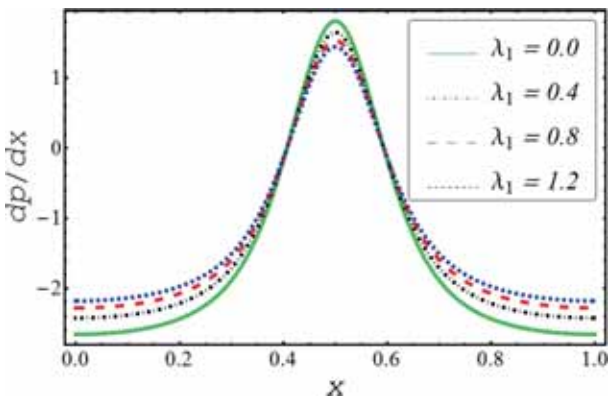

Figure 4. Variation in pressure gradient for λ_1.

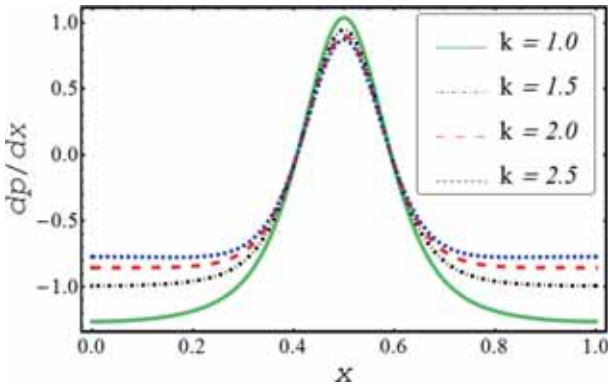

Figure 5. Variation in pressure gradient for k.

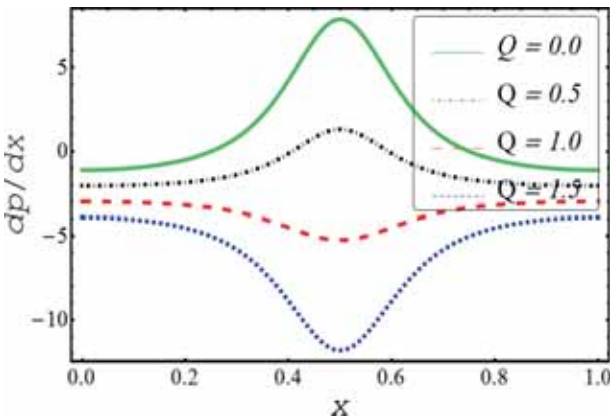

Figure 6. Variation in pressure gradient for Q.

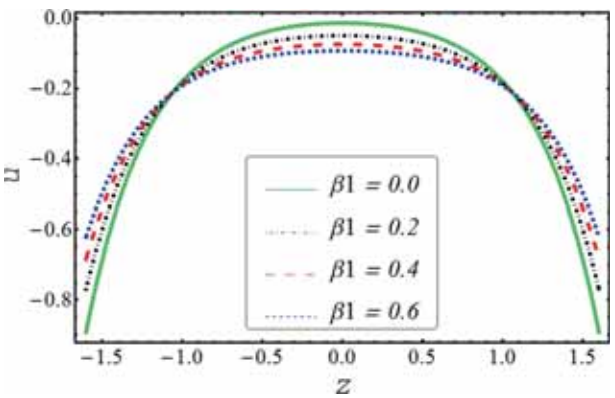

Figure 7. Change in velocity for β_1.

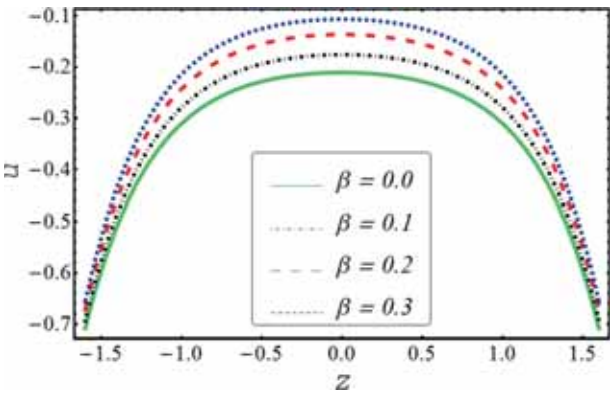

Figure 8. Change in velocity for β.

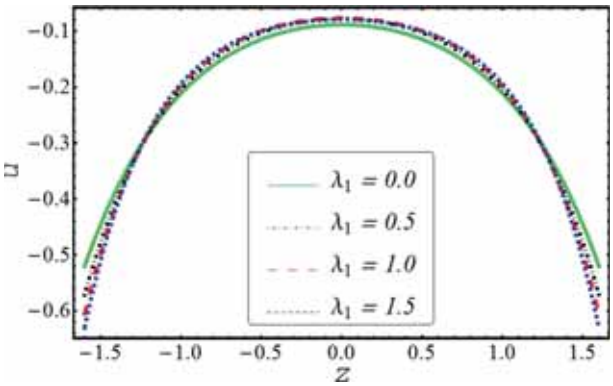

Figure 9. Change in velocity for λ_1.

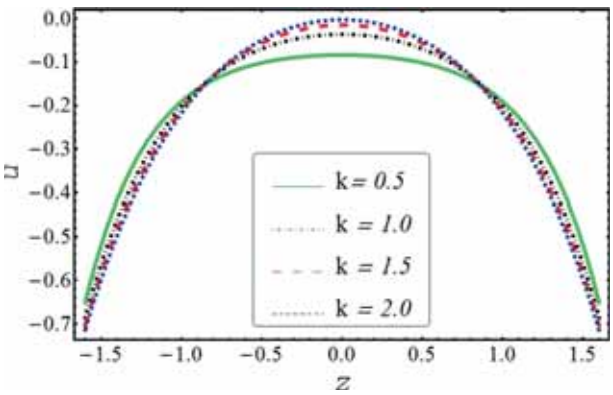

Figure 10. Change in velocity for k.

increases with increase in the value of aspect ratio β, as shown in figure 2. However, figures 3–6 show an opposite trend in the behaviour of pressure gradient. It is observed that the pressure gradient decreases by increasing values of Jeffery parameter λ_1, permeability of the porous medium k and the slip parameter β_1, except the edges of the duct where quite opposite behaviour is noted. In addition, one finds no difficulty in inferring that the pressure gradient decreases throughout the considered domain of the flow, upon increasing the numerical value of Q as shown in figure 6.

The velocity u of the peristaltic wave is displayed in figures 7–11. The slip parameter is a hindrance force in fluid flow. Therefore, the velocity of the Jeffrey fluid is interrupted when β_1 is varied, whereas the velocity of the fluid is supported by other pertinent parameters such as Jeffrey parameter, aspect ratio, volumetric flow

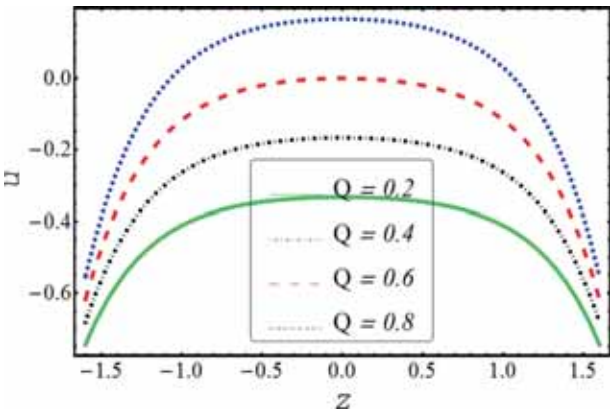

Figure 11. Change in velocity for Q.

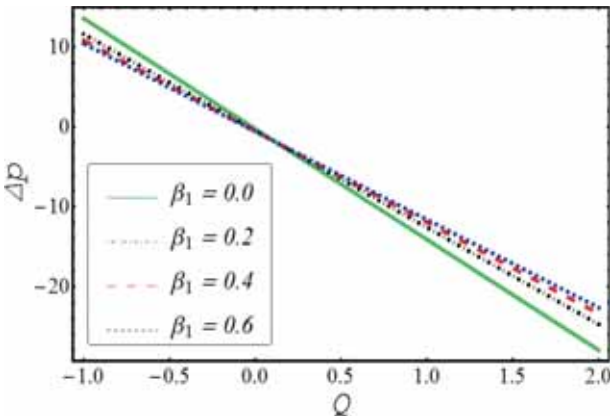

Figure 12. Change in Δp for the given numerical values of β_1.

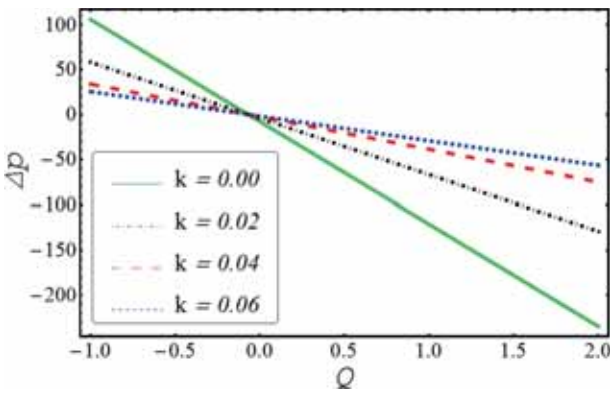

Figure 13. Change in Δp for the given numerical values of k.

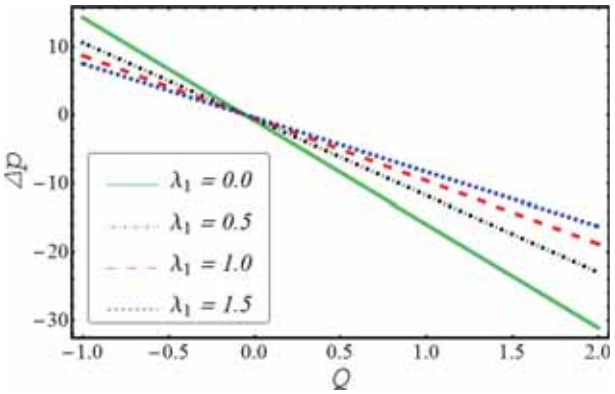

Figure 14. Change in Δp for the given numerical values of λ_1.

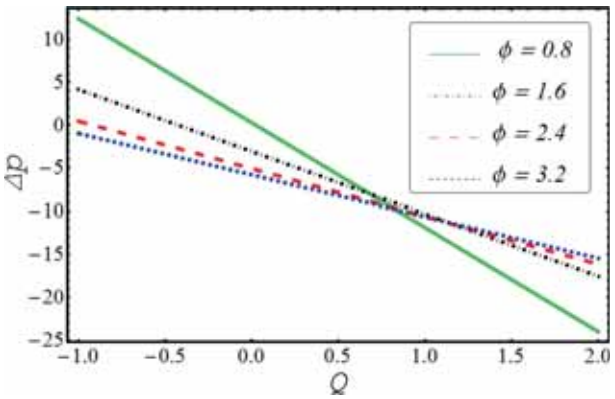

Figure 15. Change in Δp for the given numerical values of ϕ.

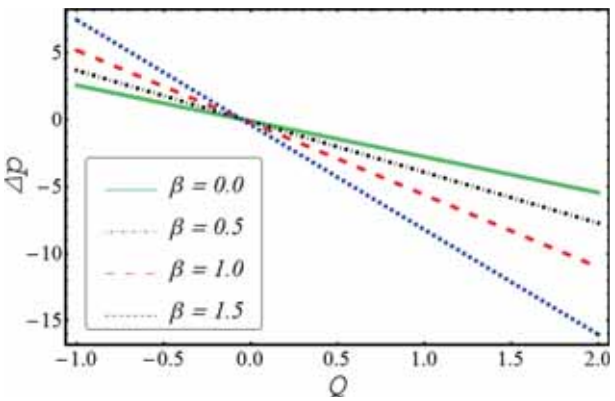

Figure 16. Change in Δp for the given numerical values of β.

rate and porosity parameters. The pressure of the fluid, at a certain point during the course of its flow, can be determined numerically, which is called pressure rise as shown in figures 12–16. It is observed that when aspect ratio increases, the pressure rise ascends its slope in the pumping region ($\Delta p > 0$) and descends in augmented region ($\Delta p < 0$). On the contrary, the behaviour of the pressure rise is much more different for the variation of volumetric flow rate, slip parameter, Jeffrey fluid parameter and permeability of the medium, as can be seen in figures 12–16.

Finally, the study of 'trapping phenomenon' is detailed here. A fluid while flowing may undergo some types of interruptions such as gravitational force, magnetic

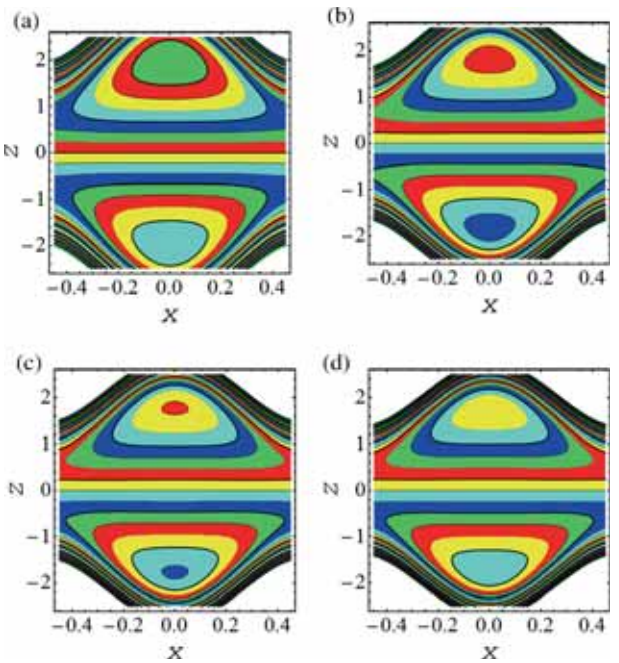

Figure 17. Display of stream lines for λ_1: (**a**) when $\lambda_1 = 0.0$, (**b**) when $\lambda_1 = 0.5$, (**c**) when $\lambda_1 = 1.0$ and (**d**) when $\lambda_1 = 1.5$.

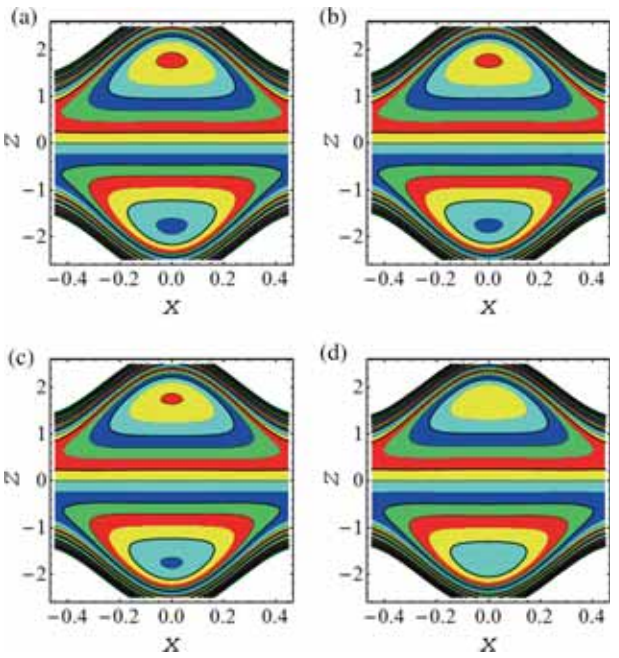

Figure 18. Display of stream lines for β: (**a**) when $\beta = 0.4$, (**b**) when $\beta = 0.7$, (**c**) when $\beta = 1.0$ and (**d**) when $\beta = 1.3$.

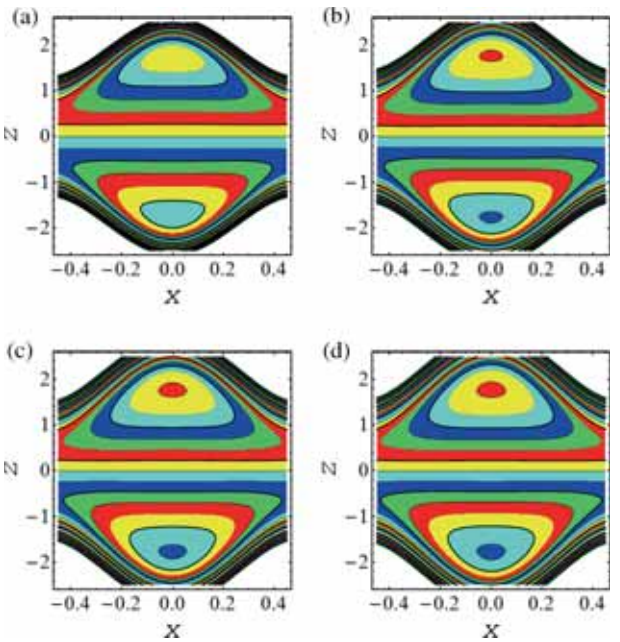

Figure 19. Display of stream lines for k: (**a**) when $k = 0.3$, (**b**) when $k = 0.6$, (**c**) when $k = 0.9$ and (**d**) when $k = 1.2$.

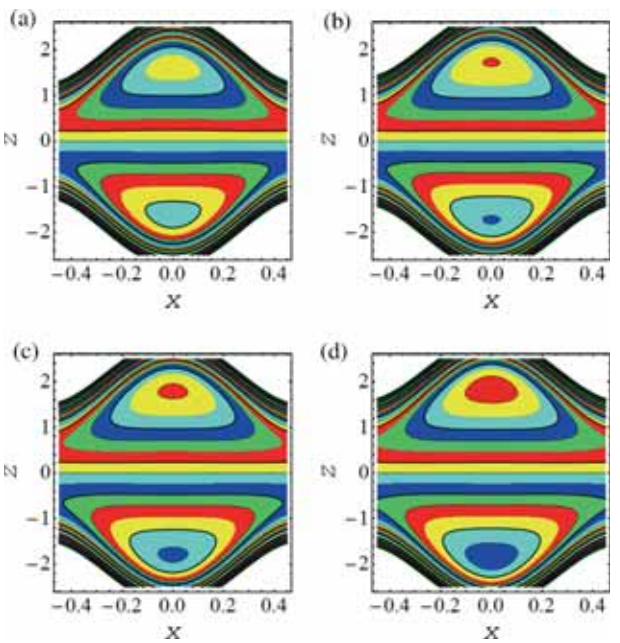

Figure 20. Display of stream lines for β_1: (**a**) when $\beta_1 = 0.0$, (**b**) when $\beta_1 = 0.3$, (**c**) when $\beta_1 = 0.6$ and (**d**) when $\beta_1 = 0.9$.

force, electric force and so on. Such hindrances are the main reasons for the appearance of boluses during the flow. The fluid near the walls of the channel or duct experiences a great deal of resistance, resulting in the shift of straight and smooth streamlines into closed ones. Hence, circulating boluses start forming and the phenomenon is known as the trapping phenomenon. Figures 17a–17d and 18a–18d display the change in streamlines as Jeffrey parameter and aspect ratio are varied, respectively. These graphs indicate that the fluid gets less troubled near the walls corresponding to the increase in λ_1 and β in numerical values, respectively. A decrease in

the number of boluses further strengthens the preceding argument that the fluid flow keeps on getting smooth and relaxed for the rise in Jeffrey parameter and aspect ratio. Nevertheless, streamlines behave differently for both porosity and slip parameter, causing enough resistance at the wall, which is evinced by the emergence of new boluses when k and β_1 are varied, as shown in figures 19a–19d and 20a–20d.

5. Conclusion

The peristaltically moving Jeffrey fluid under the combined effects of slip and porosity under the restraints of low Reynolds number and long wavelength has been examined. It is noticed that the intensity of pressure gradient keeps on reducing with the passage of time, corresponding to the higher values of slip and porosity parameters. Greater values of physical parameters increase the number of boluses. However, the trend of velocity profile for porosity parameter and slip parameter is quite different, i.e., in the respective domain as porosity parameter gets higher values, whereas the velocity of the fluid declines for the slip parameter. It is worth mentioning that by taking the non-Newtonian Jeffrey fluid parameter equal to zero, one can get the result of Newtonian fluid.

References

[1] T W Latham, *Fluid motion in peristaltic pump*, M.S. thesis (Massachusetts Institute of Technology, 1966)

[2] A H Shapiro, M Y Jaffrin and S L Weinberg, *J. Fluid Mech.* **37**(**4**), 799 (1969)

[3] S R Mahmoud, N A S Afifib and H M Al-Isedec, *Int. J. Math. Anal.* **5**(**21**), 1025 (2011)

[4] K S Mekheimer, A M Salem and A Z Zaher, *J. Egypt. Math. Soc.* **22**(**1**), 143 (2014)

[5] K Vajravelu, S Sreenadh and P Lakshminarayana, *Commun. Nonlinear Sci. Numer. Simul.* **16**(**8**), 3107 (2011)

[6] Y Abd elmaboud and K S Mekheimer, *Appl. Math. Model.* **35**(**6**), 2695 (2011)

[7] A A Khan, R Ellahi, M Mudassar Gulzar and M Sheikholeslami, *J. Magn. Magn. Mater.* **372**, 97 (2014)

[8] S Nadeem, N S Akbar and M Y Malik, *Z. Naturforsch.* **65**(**5**), 369 (2010)

[9] G M Moatimid, Y O El-Dib and M H Zekry, *Pramana – J. Phys.* **92**: 22 (2019)

[10] E F E Shehawey and W E Sebai, *Int. J. Math. Math. Sci.* **24**(**4**), 217 (2000)

[11] A Ebaid, *Phys. Lett. A* **372**(**24**), 4493 (2008)

[12] A A Khan, F Masood, R Ellahi and M M Bhatti, *J. Mol. Liq.* **258**, 186 (2018)

[13] D Tripathi, R Jhorar, O A Bég and S Shaw, *Meccanica* **53**(**8**), 2079 (2018)

[14] V K Narla, D Tripathi, O A Beg and A Kadir, *J. Eng. Math.* **111**(**1**), 127 (2018)

[15] D Tripathi, A Sharma and O A Bég, *Adv. Powder Technol.* **29**(**3**), 639 (2018)

[16] M K Chaube, A Yadav and D Tripathi, *J. Braz. Soc. Mech. Sci. Eng.* **40**(**9**), 423 (2018)

[17] M K Chaube, A Yadav, D Tripathi and O A Beg, *Korea-Aust. Rheol. J.* **30**(**2**), 89 (2018)

[18] N S Akbar, A W Butt, D Tripathi and O A Beg, *Pramana – J. Phys.* **88**: 52 (2017)

[19] M M Bhatti, A Zeeshan and R Ellahi, *Pramana – J. Phys.* **89**: 48 (2017)

[20] M Kumar, G J Reddy and N Dalir, *Pramana – J. Phys.* **91**: 60 (2018)

[21] B Mahanthesh, B J Gireesha, R S R Gorla and O D Makinde, *Neural Comput. Appl.* **30**(**5**), 1557 (2018)

[22] B J Gireesha, B Mahanthesh, R S R Gorla and P T Manjunatha, *Heat Mass Transf.* **52**(**4**), 897 (2016)

[23] B J Gireesha, B Mahanthesh, P T Manjunatha and R S R Gorla, *J. Nigerian Math. Soc.* **34**(**3**), 267 (2015)

[24] B J Gireesha, B Mahanthesh and M M Rashidi, *Int. J. Ind. Math.* **7**(**3**), 247 (2015)

[25] S Z Alamri, R Ellahi, N Shehzad and A Zeeshan, *J. Mol. Liq.* **273**, 292 (2019)

[26] A Zeeshan, N Shehzad, R Ellahi and S Z Alamri, *Neural Comput. Appl.* **30**(**11**), 3371 (2018)

[27] A Zeeshan, N Ijaz, T Abbas and R Ellahi, *Sustainability* **10**(**8**), 2671 (2018)

[28] F Hussain, R Ellahi, A Zeeshan and K Vafai, *J. Mol. Liq.* **268**, 149 (2018)

[29] C Fetecau, R Ellahi, M Khan and N A Shah, *J. Porous Media* **21**(**7**), 589 (2018)

[30] R Ellahi, S Z Alamri, A Basit and A Majeed, *J. Taibah Univ. Sci.* **12**(**4**), 476 (2018)

[31] M Hassan, M Marin, A Alsharif and R Ellahi, *Phys. Lett. A* **382**(**38**), 2749 (2018)

[32] M M Bhatti, A Zeeshan, R Ellahi and G C Shit, *Adv. Powder Technol.* **29**(**5**), 1189 (2018)

[33] R Ellahi and F Hussain, *J. Magn. Magn. Mater.* **393**, 284 (2015)

[34] R Haberman, *Applied partial differential equations: With Fourier series and boundary value problems*, 5th edn (Person-Prentice Hall, Upper Saddle River, New Jersey, USA, 2013) p. 35